Available online at www.sciencedirect.com
ScienceDirect
International Journal of Heat and Mass Transfer 50 (2007) 552–565
International Journal of HEAT and MASS TRANSFER
www.elsevier.com/locate/ijhmt

Finite circular fin method for heat and mass transfer characteristics for plain fin-and-tube heat exchangers under fully and partially wet surface conditions

Worachest Pirompugd [a,b], Chi-Chuan Wang [c], Somchai Wongwises [b,*]

[a] Department of Mechanical Engineering, Faculty of Engineering, Burapha University, Saensook, Muang, Chonburi 20131, Thailand
[b] Fluid Mechanics, Thermal Engineering and Multiphase Flow Research Lab. (FUTURE), Department of Mechanical Engineering, King Mongkut's University of Technology Thonburi, 91 Suksawas Road, 48 Bangmod, Thungkru, Bangkok 10140, Thailand
[c] Energy and Resources Lab., Industrial Technology Research Institute, Hsinchu 310, Taiwan, ROC

Received 14 December 2005; received in revised form 15 July 2006
Available online 2 October 2006

Abstract

This study proposes a new method, namely the "finite circular fin method" (FCFM), to analyze the performance of fin-and-tube heat exchangers having plain fin configuration under dehumidifying conditions. The analysis is done by dividing the heat exchanger into many tiny segments (number of tube rows × number of tube passes per row × number of fins). The tiny segments are distinguished into three types: the fully dry, partially wet or fully wet surface conditions. The proposed method is capable of handling fully and partially wet surfaces. From the test results, it is found that the sensible heat transfer performance and the mass transfer performance are insensitive to changes of fin pitch. The influence of inlet relative humidity on the sensible heat transfer performance is small, and is almost negligible when the number of tube rows is above four. For one and two row configurations, considerable increase of mass transfer performance is encountered when partially wet condition takes place. The sensible heat transfer coefficient is about the same for those in fully wet and partially wet conditions provided that the number of tube row is equal or greater than four. Correlations applicable for both fully wet and partially wet conditions are proposed to describe the heat and mass performance for the present plain fin configuration.

Keywords: Finite circular fin method; Fin-and-tube heat exchangers; Dehumidifying conditions; Sensible heat transfer performance; Mass transfer performance

1. Introduction

Fin-and-tube heat exchangers are widely used in applications of air-conditioning and refrigeration systems. They can be applicable to condensers and evaporators. In evaporators, which typically use aluminum fins with the surface temperature generally being below the dew point temperature. As a result, simultaneous heat and mass transfer occurs along the fin surfaces.

Many studies have been published on the heat and mass transfer characteristics of fin-and-tube heat exchangers under dehumidifying conditions. For instance, McQuiston [1,2] presented experimental data for five plate fin-and-tube heat exchangers, and developed a well-known heat transfer and friction correlation for both dry and wet surfaces. Mirth and Ramadhyani [3,4] investigated the heat and mass transfer characteristics of wavy fin heat exchangers. Their results showed that the Nusselt number was very sensitive to changes of the inlet dew point temperature, and that the Nusselt number decreased with an increase of dew point temperatures. Similar results were reported by Fu et al. [5] in dehumidifying heat exchangers having a louver fin configuration. They reported a pronounced decrease of the wet sensible heat transfer coefficients with the rise of the inlet relative humidity. Contrary to this, the experimental

* Corresponding author. Tel.: +66 2 470 9115; fax: +66 2 470 9111.
E-mail address: somchai.won@kmutt.ac.th (S. Wongwises).

0017-9310/$ - see front matter © 2006 Elsevier Ltd. All rights reserved.
doi:10.1016/j.ijheatmasstransfer.2006.07.017

Nomenclature

A_f surface area of fin, m^2
$A_{f,dry}$ surface area of fin of dry portion, m^2
$A_{f,wet}$ surface area of fin of wet portion, m^2
A_o total surface area, m^2
$A_{p,i}$ inside surface area of tubes, m^2
$A_{p,o}$ outside surface area of tubes, m^2
b'_p slope of the air saturation curved between the outside and inside tube wall temperature, J kg^{-1} K^{-1}
b'_r slope of the air saturation curved between the mean water temperature and the inside wall temperature, J kg^{-1} K^{-1}
$b'_{w,f}$ slope of the air saturation curved at the mean water film temperature of the fin surface, J kg^{-1} K^{-1}
$b'_{w,p}$ slope of the air saturation curved at the mean water film temperature of the tube surface, J kg^{-1} K^{-1}
$C_{p,a}$ moist air specific heat at constant pressure, J kg^{-1} K^{-1}
$C_{p,r}$ water specific heat at constant pressure, J kg^{-1} K^{-1}
D_c tube outside diameter (including collar), m
D_i tube inside diameter, m
f_r in-tube friction factors of water
F correction factor
F_p fin pitch, m
$G_{a,max}$ maximum mass velocity based on minimum flow area, kg m^{-2} s^{-1}
$h_{c,o}$ sensible heat transfer coefficient, W m^{-2} K^{-1}
$h_{d,o}$ mass transfer coefficient, kg m^{-2} s^{-1}
h_r inside heat transfer coefficient, W m^{-2} K^{-1}
I_0 modified Bessel function solution of the first kind, order 0
I_1 modified Bessel function solution of the first kind, order 1
i_a air enthalpy, J kg^{-1}
$i_{a,in}$ inlet-air enthalpy, J kg^{-1}
$i_{a,m}$ mean air enthalpy, J kg^{-1}
$i_{a,out}$ outlet-air enthalpy, J kg^{-1}
i_g saturated water vapor enthalpy, J kg^{-1}
$i_{s,f}$ saturated air enthalpy at the fin temperature, J kg^{-1}
$i_{s,f,b}$ saturated air enthalpy at the fin base temperature, J kg^{-1}
$i_{s,f,m}$ mean saturated air enthalpy at the mean fin temperature, J kg^{-1}
$i_{s,r,in}$ saturated air enthalpy at the inlet-water temperature, J kg^{-1}
$i_{s,r,m}$ mean saturated air enthalpy at the mean water temperature, J kg^{-1}
$i_{s,r,out}$ saturated air enthalpy at the outlet-water temperature, J kg^{-1}
$i_{s,p,i,m}$ mean saturated air enthalpy at the mean inside tube wall temperature, J kg^{-1}
$i_{s,p,o,m}$ mean saturated air enthalpy at the mean outside tube wall temperature, J kg^{-1}
$i_{s,w}$ saturated air enthalpy at the water film temperature, J kg^{-1}
$i_{s,w,f,m}$ mean saturated air enthalpy at the mean water film temperature of the fin surface, J kg^{-1}
j_h Chilton–Colburn j-factor of the heat transfer
j_m Chilton–Colburn j-factor of the mass transfer
K_0 modified Bessel function solution of the second kind, order 0
K_1 modified Bessel function solution of the second kind, order 1
k_f thermal conductivity of fin, W m^{-1} K^{-1}
k_r thermal conductivity of water, W m^{-1} K^{-1}
k_p thermal conductivity of tube, W m^{-1} K^{-1}
k_w thermal conductivity of water film, W m^{-1} K^{-1}
L_p tube length, m
$\dot{m}_a$ air mass flow rate, kg s^{-1}
$\dot{m}_r$ water mass flow rate, kg s^{-1}
N number of tube rows
P pressure, N m^{-2}
P_l longitudinal tube pitch, m
Pr_a Prandtl number of air
Pr_r Prandtl number of water
P_t transverse tube pitch, m
$\dot{Q}_a$ air-side heat transfer rate, W
$\dot{Q}_{avg}$ average heat transfer rate, W
$\dot{Q}_{dry,cond}$ conductive heat transfer rate for dry portion, W
$\dot{Q}_{dry,conv,max}$ convective heat transfer rate of the dry surface area that assumes the temperature of dry surface area equal to the dry/wet interface temperature, W
$\dot{Q}_{part}$ heat transfer rate for partially wet conditions, W
$\dot{Q}_{part,cond,r_i}$ conductive heat transfer rate for partially wet conditions evaluated at r_i, W
$\dot{Q}_r$ water-side heat transfer rate, W
$\dot{Q}_{wet,cond}$ conductive heat transfer rate for wet portion, W
$\dot{Q}_{wet,conv,max}$ convective heat transfer rate of wet surface area that assumes the temperature of wet surface area equal to the fin base temperature, W
$\dot{Q}'_{wet,conv,max}$ convective heat transfer rate of all surface area that assumes the temperature of all surface area equal to the fin base temperature, W
R ratio of heat transfer characteristic to mass transfer characteristic
RH relative humidity
Re_{D_i} Reynolds number of water based on inside diameter

Re_{D_c}	Reynolds number of air based on outside diameter (including collar)
r	distance from the center of the tube to the fin, m
r_i	distance from the center of the tube to the fin base, m
r_o	distance from the center of the tube to the fin tip, m
r^*	distance from the center of the tube to the interface, m
Sc_a	Schmidt number of air
Sp	fin spacing, m
T_a	temperature of air, K
$T_{a,m}$	mean temperature of air, K
T_{db}	dry-bulb temperature, K
T_{dp}	dew point temperature, K
T_f	temperature of fin, K
$T_{f,m}$	mean temperature of fin, K
$T_{f,b}$	temperature of the fin base, K
$T_{f,t}$	temperature of the fin tip, K
$T_{p,i,m}$	mean temperature of the inner tube wall, K
$T_{p,o,m}$	mean temperature of the outer tube wall, K
T_r	temperature of water, K
$T_{r,in}$	inlet-water temperature, K
$T_{r,m}$	mean temperature of water, K
$T_{r,out}$	outlet-water temperature, K
$T_{w,f,m}$	mean temperature of water film at fin surface, K
t	fin thickness, m
$U_{o,p}$	overall heat transfer coefficient based on enthalpy difference, kg m^{-2} s^{-1}
V_r	velocity of water, m s^{-1}
W_a	humidity ratio of moist air, kg kg^{-1}
$W_{a,m}$	mean air humidity ratio, kg kg^{-1}
$W_{s,p,o,m}$	mean saturated air humidity ratio at the mean outside tube wall temperature, kg kg^{-1}
$W_{s,w}$	saturated air humidity ratio at the water film temperature, kg kg^{-1}
$W_{s,w,f,m}$	mean saturated air humidity ratio at the mean water film temperature of the fin surface, kg kg^{-1}
y_w	thickness of condensate water film, m
$\eta_{f,dry}$	fully dry fin efficiency
$\eta_{f,part}$	partially wet fin efficiency
$\eta'_{f,part}$	effectively partially wet fin efficiency
$\eta_{f,wet}$	fully wet fin efficiency
μ_r	dynamic viscosity of water, N s m^{-2}
ρ_r	mass density of water, kg m^{-3}
θ_{dry}	air temperature difference, K
θ_{dry,r^*}	air temperature difference at r^*, K
θ_{wet}	air enthalpy difference, J kg^{-1}
θ_{wet,r_i}	air enthalpy difference at r_i, J kg^{-1}

data of Seshimo et al. [6] indicated that the Nusselt number was relatively independent of the inlet conditions. Wang et al. [7] studied the effects of the fin pitch, the number of tube rows, and the inlet relative humidity on the heat transfer performance under dehumidification, they concluded that the sensible heat transfer performance is relatively independent of the inlet humidity. The differences in the existing literature are attributed to the different reduction methodologies. Lage [8] presented the numerical model for simulating the heat transfer process of air flowing in between two parallel fins of a finned-tube heat exchanger. The numerical simulation detected the existence of tube-to-tube heat transfer and the corresponding detrimental impact it might have on the overall capacity of the heat transfer. It was found that the tube-to-tube heat transfer affected the overall capacity and was shown to account for approximately 20% of the heat exchanger capacity. Shih [9] applied the computational fluid dynamics (CFD) for predicting the heat transfer performance on the air side of a domestic refrigerator evaporator. The numerical results showed that the non-uniformities and flow maldistributions could deteriorate the overall heat transfer performance of evaporator. Tutar and Akkoca [10] studied three-dimensional time-dependent modeling of unsteady laminar flow and heat transfer over single and multi row plate fin-and-tube heat exchangers. It was found that the numerical results for the integral heat transfer parameters agreed well with available experimental measurements. Pirompugd et al. [11,12] presented a new reduction method for the calculation of the heat and mass transfer characteristics for fin-and-tube heat exchangers under dehumidifying conditions. Their results showed that the heat and mass transfer characteristics were relatively independent of fin pitch and of relative humidity.

In practice, the fin surfaces may be fully wet, fully dry or partially wet depending on the difference between dew point temperature and surface temperature. Notice that if the outer tube surface (including collar) temperature is higher than the dew point temperature of moist air, there is only sensible heat transfer and is termed as fully dry condition. However, if the fin tip temperature is lower than the dew point temperature of moist air, sensible and latent heat transfer occur at the same time for all fin surfaces. This condition is regarded as the fully wet condition. Occasionally, part of the fin tip temperature is higher than the dew point temperature whereas the rest of fin surface temperature is lower than the dew point temperature in such condition the partially wet surface is seen. There are a number of papers addressing the heat transfer performance of the heat exchangers under partially wet surface conditions. Recently, Xia and Jacobi [13] formulated the logarithmic-mean temperature difference (LMTD) and logarithmic-mean enthalpy difference (LMED) methods for fully dry, fully wet, partially wet and frosted surface conditions.

It can be noted that almost all of the theoretical and experimental investigations found in literature were paid attention on the heat transfer characteristics, research on the mass transfer characteristics under partially wet surface

condition is still limited. As a consequence, the objective of this study to provide a detailed method for analyzing the heat and mass transfer performances of fin-and-tube heat exchangers under partially wet surfaces conditions. A new method, namely the "finite circular fin method" (FCFM), is proposed to analyze the performance of the heat exchangers having plain fin configuration under dehumidifying conditions.

2. Experimental apparatus

The schematic diagram of the experimental air circuit assembly is shown in Fig. 1. It consists of a closed-loop wind tunnel in which air is circulated by a variable speed centrifugal fan (7.46 kW, 10 HP). The air duct is made of galvanized sheet steel and has an 850 mm × 550 mm cross-section. The dry-bulb and wet-bulb temperatures of the inlet-air are controlled by an air-ventilator that can provide a cooling capacity of up to 21.12 kW (6RT). The air flow rate measurement station is an outlet chamber set up with multiple nozzles. This setup is based on the ASHRAE 41.2 standard [14]. A differential pressure transducer is used to measure the pressure difference across the nozzles. The air temperatures at the inlet and exit zones across the sample heat exchangers are measured by two psychrometric boxes based on the ASHRAE 41.1 standard [15].

The working medium for the tube side is cold water. A thermostatically controlled reservoir provides cold water at selected temperatures. The temperature differences on the water side are measured by two precalibrated RTDs. The water volumetric flow rate is measured by a magnetic flow meter with a ±0.001 L/s precision. All the temperature measuring probes are resistance temperature devices (Pt100), with a calibrated accuracy of ±0.05 °C. In the experiments, only the data that satisfy the ASHRAE 33-78 [16] requirements (namely, the energy balance condition, $|\dot{Q}_r - \dot{Q}_a|/\dot{Q}_{avg}$, is less than 0.05, where $\dot{Q}_a$, $\dot{Q}_r$ and $\dot{Q}_{avg}$ are the air-side heat transfer rate, water-side heat transfer rate and average heat transfer rate between air-side and water-side, respectively) are considered in the final analysis. Detailed geometry used for the present plain fin-and-tube heat exchangers is tabulated in Table 1. The test fin-and-tube heat exchangers are tension wrapped having a "L" type fin collar. The test conditions of the inlet-air are as follow:

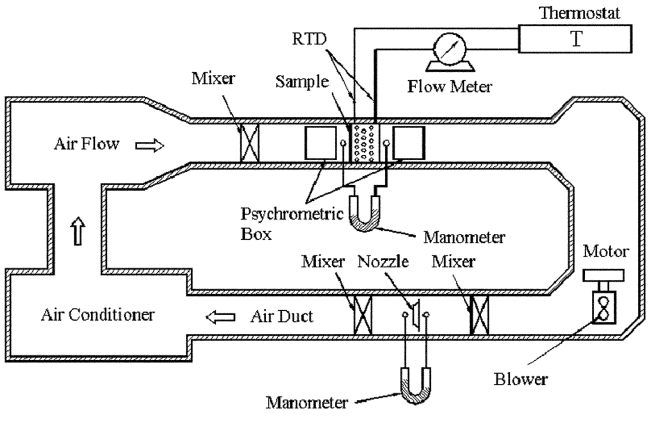

Fig. 1. Schematic diagram of experimental apparatus.

Table 1
Geometric dimensions of the plain fin-and-tube heat exchangers

No.	F_p (m)	t (m)	D_c (m)	P_t (m)	P_l (m)	N
1	0.00119	0.000115	0.00851	0.0254	0.0191	1
2	0.00175	0.000120	0.01034	0.0254	0.0220	1
3	0.00204	0. 000115	0.00851	0.0254	0.0191	1
4	0.00223	0. 000115	0.01023	0.0254	0.0191	1
5	0.00250	0. 000120	0.01034	0.0254	0.0220	1
6	0.00120	0. 000115	0.00693	0.0177	0.0136	1
7	0.00121	0. 000115	0.00693	0.0177	0.0136	1
8	0.00198	0. 000115	0.00693	0.0177	0.0136	1
9	0.00199	0. 000115	0.00693	0.0177	0.0136	1
10	0.00123	0. 000115	0.00851	0.0254	0.0191	2
11	0.00170	0. 000120	0.00862	0.0254	0.0191	2
12	0.00206	0. 000115	0.00851	0.0254	0.0191	2
13	0.00224	0. 000130	0.01023	0.0254	0.0220	2
14	0.00320	0. 000130	0.01023	0.0254	0.0220	2
15	0.00122	0. 000115	0.00753	0.0210	0.0127	2
16	0.00122	0. 000115	0.00753	0.0210	0.0127	2
17	0.00123	0. 000115	0.01023	0.0254	0.0191	2
18	0.00178	0. 000115	0.00753	0.0210	0.0127	2
19	0.00179	0. 000115	0.00753	0.0210	0.0127	2
20	0.00182	0. 000130	0.01023	0.0254	0.0220	2
21	0.00313	0. 000120	0.00862	0.0254	0.0191	2
22	0.00123	0. 000115	0.01023	0.0254	0.0191	4
23	0.00155	0. 000115	0.01023	0.0254	0.0191	4
24	0.00203	0. 000130	0.01023	0.0254	0.0220	4
25	0.00223	0. 000130	0.01023	0.0254	0.0220	4
26	0.00300	0. 000130	0.01023	0.0254	0.0220	4
27	0.00121	0. 000115	0.00851	0.0254	0.0191	4
28	0.00122	0. 000115	0.00753	0.0210	0.0127	4
29	0.00160	0. 000115	0.00851	0.0254	0.0191	4
30	0.00170	0. 000120	0.00862	0.0254	0.0191	4
31	0.00178	0. 000115	0.00753	0.0210	0.0127	4
32	0.00231	0. 000115	0.01023	0.0254	0.0191	4
33	0.00313	0. 000120	0.00862	0.0254	0.0191	4
34	0.00185	0. 000130	0.01023	0.0254	0.0220	6
35	0.00221	0. 000130	0.01023	0.0254	0.0220	6
36	0.00316	0. 000130	0.01023	0.0254	0.0220	6

Dry-bulb temperature of the air	27 ± 0.5 °C
Inlet relative humidity for the incoming air	50% and 90%
Inlet-air velocity	From 0.3 to 4.5 m/s
Inlet-water temperature	7 ± 0.5 °C
Water velocity inside the tube :	1.5–1.7 m/s
Tube-side Reynolds number :	6900–20,400

The test conditions approximate those encountered with typical fan-coils and evaporators of air-conditioning applications. Uncertainties reported in the present investigation, following the single-sample analysis proposed by Moffat [17], are tabulated in Table 2.

Table 2
Summary of estimated uncertainties

Primary measurements		Derived quantities		
Parameter	Uncertainty (%)	Parameter	Uncertainty $Re_{Dc} = 400$ (%)	Uncertainty $Re_{Dc} = 5000$ (%)
$\dot{m}_a$	0.3–1	Re_{Dc}	±1.0	±0.57
$\dot{m}_r$	0.5	Re_{Di}	±0.73	±0.73
ΔP	0.5	$\dot{Q}_r$	±3.95	±1.22
T_r	0.05 K	$\dot{Q}_a$	±5.5	±2.4
T_a	0.1 K	j_h, j_m	±11.4	±5.9

3. Data reduction

3.1. Heat transfer coefficient ($h_{c,o}$)

The total heat transfer rate used in the calculation is the average of $\dot{Q}_a$ and $\dot{Q}_r$, namely,

$$\dot{Q}_a = \dot{m}_a(i_{a,in} - i_{a,out}) \quad (1)$$

$$\dot{Q}_r = \dot{m}_r C_{p,r}(T_{r,out} - T_{r,in}) \quad (2)$$

$$\dot{Q}_{avg} = \frac{\dot{Q}_a + \dot{Q}_r}{2} \quad (3)$$

In this study, a new reduction method, namely the "finite circular fin method (FCFM)" is proposed for detailed evaluation of the performance of fin-and-tube heat exchanger instead of conventional lump approach. The proposed method is capable of handling test results for both fully wet and partially wet conditions. Analysis of the fin-and-tube heat exchanger is firstly carried out by dividing the heat exchanger into many tiny segments (number of tube rows × number of tube passes per row × number of fins) as shown in Fig. 2(a). For calculation of the fin efficiency, the equivalent circular area method as shown in Fig. 2(b) is adopted. The tiny segments can be distinguished into three types. The first one is the fully dry condition, as shown in Fig. 2(c.1), in which the outside tube (including collar) temperature is higher than the dew point temperature of the moist air. As a result, only sensible heat transfer occurs on the whole area of this tiny segment. The second case is the fully wet condition, as shown in Fig. 2(c.2), in which the fin tip temperature is lower than the dew point temperature of moist air. Both sensible and latent heat transfer takes place along the area of each tiny segment. The last one is the partially wet condition, as shown in Fig. 2(c.3), in which the outside tube (including collar) temperature is lower than the dew point temperature of the moist air but the fin tip temperature is higher. Therefore the region of $r_i \leqslant r \leqslant r^*$ is fully wet condition whereas it is fully dry in $r^* \leqslant r \leqslant r_0$. In this study, we had proposed a reduction method that can resolve these three cases. Detailed reduction method for the fully dry and fully wet conditions can be found from previous studies [18,11,12] and will not be repeated here. Only the reduction method applicable for partially wet condition will be addressed hereafter.

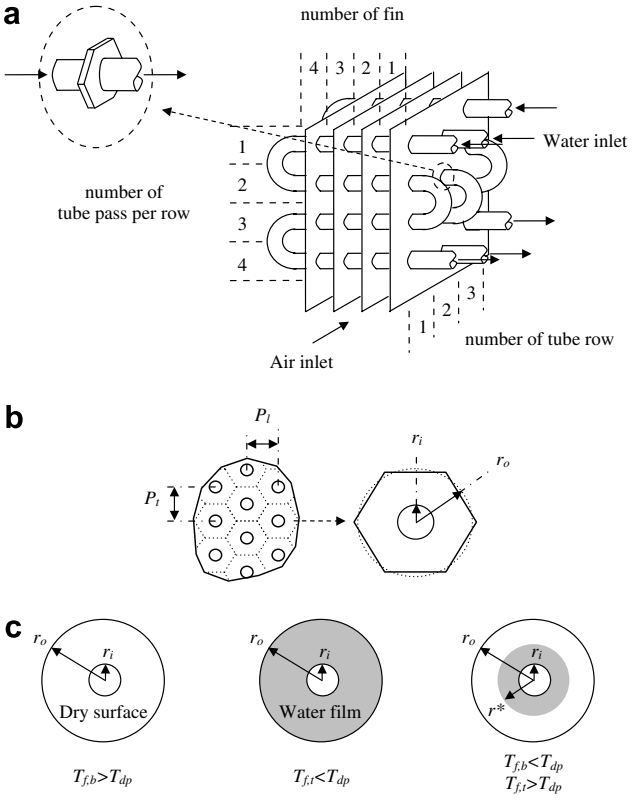

Fig. 2. Finite circular fin method. (a) Schematic of the fin-and-tube heat exchanger used for data reduction. (b) Equivalent circular area method. (c) Circular fin in fully dry, fully wet and partially wet conditions.

3.2. Reduction method for partially wet condition

The overall heat transfer coefficient, $U_{o,p}$, is based on the enthalpy potential and is given as follows:

$$\dot{Q}_{part} = U_{o,p} A_o \Delta i_m F \quad (4)$$

where Δi_m is the mean enthalpy difference for a counter flow coil,

$$\Delta i_m = i_{a,m} - i_{s,r,m} \quad (5)$$

According to Bump [19] and Myers [20], for the counter flow configuration, the mean enthalpy is

$$i_{a,m} = i_{a,in} + \frac{i_{a,in} - i_{a,out}}{\ln\left(\frac{i_{a,in} - i_{s,r,out}}{i_{a,out} - i_{s,r,in}}\right)} - \frac{(i_{a,in} - i_{a,out})(i_{a,in} - i_{s,r,out})}{(i_{a,in} - i_{s,r,out}) - (i_{a,out} - i_{s,r,in})} \quad (6)$$

$$i_{s,r,m} = i_{s,r,out} + \frac{i_{s,r,out} - i_{s,r,in}}{\ln\left(\frac{i_{a,in} - i_{s,r,out}}{i_{a,out} - i_{s,r,in}}\right)} - \frac{(i_{s,r,out} - i_{s,r,in})(i_{a,in} - i_{s,r,out})}{(i_{a,in} - i_{s,r,out}) - (i_{a,out} - i_{s,r,in})} \quad (7)$$

For the FCFM, F is the correction factor accounting for a single-pass, cross-flow heat exchanger for one fluid mixed, the other fluid being unmixed, as described by Threlkeld [21]. The overall heat transfer coefficient is related to the individual heat transfer resistance as follows:

$$\frac{1}{U_{o,p}} = \frac{b'_r A_o}{h_r A_{p,i}} + \frac{b'_p A_o \ln\left(\frac{D_o}{D_i}\right)}{2\pi k_p L_p} + \frac{1}{h_{o,w}\left(\frac{A_{p,o}}{b'_{w,p} A_o} + \frac{A_f \eta'_{f,part}}{b'_{w,f} A_o}\right)} \tag{8}$$

where

$$h_{o,w} = \frac{1}{\frac{C_{p,a}}{b'_{w,f} h_{c,o}} + \frac{y_w}{k_w}} \tag{9}$$

y_w in Eq. (9) is the thickness of the water film. A constant of 0.005 in. was proposed by Myers [20]. The water-side heat transfer coefficient, h_r is evaluated with the Gnielinski correlation [22],

$$h_r = \frac{(f_r/2)(Re_{D_i} - 1000)Pr_r}{1.07 + 12.7\sqrt{f_r/2}(Pr_r^{2/3} - 1)} \cdot \frac{k_r}{D_i} \tag{10}$$

and the friction factor, f_r is

$$f_r = \frac{1}{(1.58 \ln Re_{D_i} - 3.28)^2} \tag{11}$$

The Reynolds number used in Eqs. (10) and (11) is determined from $Re_{D_i} = \rho_r V_r D_i/\mu_r$. It is based on the inside diameter of the tube. Eqs. (10) and (11) can be satisfyingly applied with the flow when $Re_{D_i} > 2300$.

In Eq. (8) there are four quantities (b'_r, b'_p, $b'_{w,p}$ and $b'_{w,f}$) involving enthalpy-temperature ratios that must be evaluated. The quantities of b'_r and b'_p can be calculated as

$$b'_r = \frac{i_{s,p,i,m} - i_{s,r,m}}{T_{p,i,m} - T_{r,m}} \tag{12}$$

$$b'_p = \frac{i_{s,p,o,m} - i_{s,p,i,m}}{T_{p,o,m} - T_{p,i,m}} \tag{13}$$

the values of $b'_{w,p}$ and $b'_{w,f}$ are the slopes of saturated air enthalpy curves evaluated at the mean water film temperature at the base surface and the fin surface, respectively. Without loss of generality, $b'_{w,p}$ can be approximated by the slope of the saturated air enthalpy curve evaluated at the base surface temperature [7]. Evaluation of $b'_{w,f}$ requires a trial and error procedure. For the trial and error procedure, $i_{s,w,f,m}$ must be calculated using the following equation:

$$i_{s,w,f,m} \approx i_{a,m} - \frac{C_{p,a} h_{o,w} \eta'_{f,part}}{b'_{w,f} h_{c,o}} \times \left(1 - U_{o,p} A_o \left[\frac{b'_r}{h_r A_{p,i}} + \frac{b'_p \ln\left(\frac{D_o}{D_i}\right)}{2\pi k_p L_p}\right]\right)(i_{a,m} - i_{s,r,m}) \tag{14}$$

Hence, the corresponding fin efficiency is calculated by the equivalent circular area method as depicted in Fig. 2(b). Kern and Kraus [23] proposed the differential equation and its solution for the fully dry condition. For a partially wet circular fin, as shown in Fig. 2(c.3), neglecting the heat transfer through the fin tip, the differential equation for the dry fin portion ($r^* \leqslant r \leqslant r_o$) in terms of temperature excess $\theta_{dry} = T_{a,m} - T_f$ is

$$r^2 \frac{d^2\theta_{dry}}{dr^2} + r\frac{d\theta_{dry}}{dr} - M_m^2 r^2 \theta_{dry} = 0 \tag{15}$$

The associated solution is as follows:

$$\theta_{dry} = \theta_{dry,r^*}\left[\frac{K_1(M_m r_o)I_0(M_m r) + I_1(M_m r_o)K_0(M_m r)}{K_1(M_m r_o)I_0(M_m r^*) + I_1(M_m r_o)K_0(M_m r^*)}\right] \tag{16}$$

where

$$M_m = \sqrt{\frac{2h_{c,o}}{k_f t}} \tag{17}$$

and θ_{dry,r^*} is the temperature excess evaluated at r^*.

For the equation and solution applicable to the wet fin portion ($r_i \leqslant r \leqslant r^*$), the enthalpy excess ($\theta_{wet} = i_{a,m} - i_{s,f}$) is used as the primary variable:

$$r^2 \frac{d^2\theta_{wet}}{dr^2} + r\frac{d\theta_{wet}}{dr} - M_T^2 r^2 \theta_{wet} = 0 \tag{18}$$

where

$$M_T = \sqrt{\frac{2h_{o,w}}{k_f t}} \tag{19}$$

Subject to the boundary conditions,

$$\theta_{wet}|_{r=r_i} = \theta_{wet,r_i} \tag{20}$$

$$\dot{Q}_{wet,cond}\big|_{r=r^*} = \dot{Q}_{dry,cond}\big|_{r=r^*} \tag{21}$$

where θ_{wet,r_i} is the enthalpy excess evaluated at r_i.

The second boundary condition, in which the conduction heat transfer rate continues at the wet/dry boundary of r^*, yielding:

$$\left.\frac{d\theta_{wet}}{dr}\right|_{r=r^*} = b'_{w,f}\left.\frac{d\theta_{dry}}{dr}\right|_{r=r^*} \tag{22}$$

The solution of the differential equation of Eq. (18) is

$$\theta_{wet} = \frac{\alpha I_0(M_T r) + \beta K_0(M_T r)}{M_T I_1(M_T r^*)K_0(M_T r_i) + M_T I_0(M_T r_i)K_1(M_T r^*)} \tag{23}$$

where

$$\alpha = \theta_{wet,r_i} M_T K_1(M_T r^*) + \gamma K_0(M_T r_i) \tag{24}$$

$$\beta = \theta_{wet,r_i} M_T I_1(M_T r^*) - \gamma I_0(M_T r_i) \tag{25}$$

$$\gamma = b'_{w,f}\theta_{dry,r^*} M_m \times \left[\frac{K_1(M_m r_o)I_1(M_m r^*) - I_1(M_m r_o)K_1(M_m r^*)}{K_1(M_m r_o)I_0(M_m r^*) + I_1(M_m r_o)K_0(M_m r^*)}\right] \tag{26}$$

Eq. (26) can be applied to the fully wet condition by assigning r_o to r^*. The partially wet fin efficiency can be written as

$$\eta_{f,part} = \frac{\dot{Q}_{part,cond,r_i}}{\dot{Q}_{wet,conv,max} + \dot{Q}_{dry,conv,max}} \quad (27)$$

where $\dot{Q}_{part,cond,r_i}$ is the heat transfer rate evaluated at r_i, $\dot{Q}_{wet,conv,max}$ is the convective heat transfer rate of wet surface area that assumes the temperature of wet surface equal to fin base temperature whereas $\dot{Q}_{dry,conv,max}$ is the convective heat transfer rate of the dry portion that assumes the temperature of dry surface equal to the dry/wet interface temperature that is in fact equal to the dew point temperature. However, the partially wet fin efficiency obtained from Eq. (27) is not applicable for the Threlkeld's method. Because the heat transfer rate from Threlkeld's method is based on the enthalpy difference and can not directly applied to Eq. (27). In that respect, we had defined the effectively partially wet fin efficiency based on the enthalpy difference, and is given as

$$\eta'_{f,part} = \frac{\dot{Q}_{part,cond,r_i}}{\dot{Q}'_{wet,conv,max}} = \frac{\dot{Q}_{wet,conv,max} + \dot{Q}_{dry,conv,max}}{\dot{Q}'_{wet,conv,max}} \eta_{f,part} \quad (28)$$

where $\dot{Q}'_{wet,conv,max}$ is the convective heat transfer rate that assumes the temperature of all surface area equal to the fin base temperature. Then, the partially wet fin efficiency is

$$\eta_{f,part} = \frac{2r_i}{M_T(r^{*2} - r_i^2)\theta_{wet,r_i} + M_T C_{p,a}\theta_{dry,r^*}(r_o^2 - r^{*2})} \times \left[\frac{\beta K_1(M_T r_i) - \alpha I_1(M_T r_i)}{M_T I_1(M_T r^*)K_0(M_T r_i) + M_T I_0(M_T r_i)K_1(M_T r^*)}\right] \quad (29)$$

and the effectively partially wet fin efficiency is given as

$$\eta'_{f,part} = \left(\frac{r^{*2} - r_i^2}{r_o^2 - r_i^2} + C_{p,a}\frac{\theta_{dry,r^*}}{\theta_{wet,r_i}}\frac{r_o^2 - r*^2}{r_o^2 - r_i^2}\right)\eta_{f,part} \quad (30)$$

Eq. (30) can be applied to the fully wet condition by assigning r_o to r^*. An algorithm for calculation of the partially wet condition is given as follows:

1. Calculate the tube-side heat transfer coefficient of h_r using Eq. (10).
2. Assume an outlet-air enthalpy of the calculated segment.
3. Calculate $i_{a,m}$ by Eq. (6) and $i_{s,r,m}$ by Eq. (7).
4. Assume values of $T_{p,i,m}$ and $T_{p,o,m}$.
5. Calculate $\frac{b'_r A_o}{h_r A_{p,i}}$ and $\frac{b'_p A_o \ln\left(\frac{D_c}{D_i}\right)}{2\pi k_p L_p}$.
6. Assume $T_{w,f,m}$.
7. Assume r^*.
8. Calculate θ_{wet} at r^* by Eq. (23).
9. Calculate $i_{s,f}$ from θ_{wet} at r^*.
10. Calculate T_f from $i_{s,f}$ at r^*.
11. If T_f obtained in step 10 is not equal to the dew point temperature of the moist air, the calculation steps 8–10 will be repeated with a new r^* until T_f is equal to the dew point temperature.
12. Calculate the $\eta_{f,part}$ and $\eta'_{f,part}$ using Eqs. (29) and (30), respectively.
13. Calculate $U_{o,p}$ from Eq. (8).
14. Calculate $i_{s,w,f,m}$ by Eq. (14).
15. Calculate $T_{w,f,m}$ from $i_{s,w,f,m}$.
16. If $T_{w,f,m}$ obtained in step 15 is not equal to that assumed in step 6, the calculation steps 7–15 will be repeated with $T_{w,f,m}$ obtained in step 15 until $T_{w,f,m}$ is constant.
17. Calculate $\dot{Q}_{part}$ from Eq. (4) of this segment.
18. Calculate $T_{p,i,m}$ and $T_{p,o,m}$ from the inside convection heat transfer rate and the conduction heat transfer rate.
19. If $T_{p,i,m}$ and $T_{p,o,m}$ obtained in step 18 are not equal to those assumed in step 4, the calculation steps 5–18 will be repeated with $T_{p,i,m}$ and $T_{p,o,m}$ obtained in step 18 until $T_{p,i,m}$ and $T_{p,o,m}$ are constant.
20. Calculate the outlet-air enthalpy and the outlet-water temperature from $\dot{Q}_{wet}$ obtained in step 17.
21. If the outlet-air enthalpy obtained in step 20 is not equal to that assumed in step 2, the calculation steps 3–20 will be repeated with the outlet-air enthalpy obtained in step 20 until the outlet-air enthalpy is constant.

In this study, detailed evaluation algorithm of the heat transfer coefficient $h_{c,o}$ with the present FCFM relative to conventional lump approach is given as follows:

1. Calculate the moist air-side heat transfer rate and the water-side heat transfer rate by Eqs. (1) and (2), respectively.
2. Calculate the total heat transfer rate from Eq. (3).
3. Assume $h_{c,o}$ for all segments.
4. Calculate the heat transfer performance for each segment with the following procedures.
   (a) Calculate the dew point temperature.
   (b) Assign $T_{r,m}$ to $T_{p,i,m}$ and $T_{p,o,m}$.
   (c) Calculate the fin tip temperature for the fully wet condition (using Eq. (23) by assigning r_o to r^*).
   (d) If $T_{p,o,m}$ is higher than the dew point temperature, the algorithm of the fully dry condition is done.
   (e) If the fin tip temperature is lower than the dew point temperature, the algorithm of the fully wet condition is adopted (see [11,12]).
   (f) If $T_{p,o,m}$ is lower than the dew point temperature but the fin tip temperature is higher than the dew point temperature, the algorithm of the partially wet condition is used.
   (g) If $T_{p,i,m}$ and $T_{p,o,m}$ obtained in steps 4(d)–4(f) are not equal to those assumed in step 4(b), the calculation steps 4(c)–4(f) will be repeated with $T_{p,i,m}$ and $T_{p,o,m}$ obtained in steps 4(d)–4(f) until $T_{p,i,m}$ and $T_{p,o,m}$ are constants.

5. If the summation of the heat transfer rate for all elements is not equal to the total heat transfer rate obtained in step 2, $h_{c,o}$ will be assumed with a new value and the calculation step 4 will be repeated until the summation of the heat transfer rate for all elements is equal to the total heat transfer rate.

3.3. Mass transfer coefficient ($h_{d,o}$)

The cooling and dehumidifying of moist air by a cold surface involves simultaneously heat and mass transfer, and can be described by the process line equation from Threlkeld [21]:

$$\frac{di_a}{dW_a} = R\frac{(i_a - i_{s,w})}{(W_a - W_{s,w})} + (i_g - 2501R) \tag{31}$$

where R represents the ratio of heat transfer characteristic to mass transfer characteristic.

$$R = \frac{h_{c,o}}{h_{d,o}C_{p,a}} \tag{32}$$

However, Eq. (31) did not correctly describe the dehumidification process on the psychrometric chart for the present fin-and-tube heat exchanger. This is because the saturated air enthalpy ($i_{s,w}$) at the mean temperature at the fin surface is different from that at the fin base. In this regard, a modification of the process line on the psychrometric chart corresponding to the fin-and-tube heat exchanger is made. In this study, we had proposed a method to resolve the partially wet condition. Detailed reduction method for the fully wet conditions can be found from previous studies [11,12] and will not be repeated here. From the energy balance of dehumidification one can arrive at the following expression:

$$\dot{m}_a di_a = \frac{h_{c,o}}{C_{p,a}} dA_{p,o}(i_{a,m} - i_{s,p,o,m}) + \frac{h_{c,o}}{C_{p,a}} dA_{f,wet}(i_{a,m} - i_{s,w,f,m}) + h_{c,o} dA_{f,dry}(T_{a,m} - T_{f,m}) \tag{33}$$

Note that the first term on the right hand side denotes the heat transfer from the outside tube, the second term represents the heat transfer from wet part of the fin and the third term is the sensible heat transfer from dry part of fin. Conservation of mass of the water condensate leads to:

$$\dot{m}_a dW_a = h_{d,o} dA_{p,o}(W_{a,m} - W_{s,p,o,m}) + h_{d,o} dA_{f,wet}(W_{a,m} - W_{s,w,f,m}) \tag{34}$$

Dividing Eq. (33) by Eq. (34) yields

$$\frac{di_a}{dW_a} = \frac{R\cdot(i_{a,m} - i_{s,p,o,m}) + R\cdot\left(\frac{r^{*2} - r_i^2}{r_o^2 - r_i^2}\right)\cdot(\varepsilon - 1)\cdot(i_{a,m} - i_{s,w,f,m}) + R\cdot\left(\frac{r_o^2 - r^{*2}}{r_o^2 - r_i^2}\right)\cdot(\varepsilon - 1)\cdot C_p(T_{a,m} - T_{f,m})}{(W_{a,m} - W_{s,p,o,m}) + \left(\frac{r^{*2} - r_i^2}{r_o^2 - r_i^2}\right)\cdot(\varepsilon - 1)\cdot(W_{a,m} - W_{s,w,f,m})} \tag{35}$$

where

$$\varepsilon = \frac{A_o}{A_{p,o}} \tag{36}$$

By assuming a value of R, Eq. (35) can be easily integrated via the following iterative algorithm. The mass transfer coefficient can be obtained accordingly. Procedures for obtaining the mass transfer coefficients for the partially wet condition are given in the following:

1. Obtain $W_{s,p,o,m}$ and $W_{s,w,f,m}$ from $i_{s,p,o,m}$ and $i_{s,w,f,m}$ from the calculations of heat transfer.
2. Assume a value of R.
3. Calculations are performed from the first element to the last element, employing the following procedures:
   (a) Assume a humidity ratio at the exit of heat exchanger.
   (b) Calculate the outlet humidity ratio of each element by Eq. (35).
   (c) If the calculated outlet humidity ratio obtained from step 3(b) is not equal to the assumed value from step 3(a), repeat the calculation step 3(b).
4. If the summation of the outlet-air humidity ratio for each element of the last row is not equal to the measured outlet-air humidity ratio, assume a new R value and repeat the calculation step 3 until the summation of the outlet humidity ratio of the last row is equal to the measured outlet humidity ratio.

In this study, the FCFM for detailed evaluation of the performance of fin-and-tube heat exchanger is proposed instead of the conventional lump approach. An algorithm for solving the mass coefficient $h_{d,o}$ is given as follows:

1. If $T_{p,o,m}$ is higher than the dew point temperature. The outlet humidity ratio is equal to the inlet humidity ratio.
2. If the fin tip temperature is lower than the dew point temperature, the algorithm of the fully wet condition is employed.
3. If $T_{p,o,m}$ is lower than the dew point temperature but the fin tip temperature is higher than the dew point temperature, the algorithm of the partially wet condition is done.

3.4. Chilton–Colburn j-factor for heat and mass transfer (j_h and j_m)

The heat and mass transfer characteristics of the heat exchanger is presented by the following non-dimensional group:

$$j_h = \frac{h_{c,o}}{G_{a,max} C_{p,a}} Pr_a^{2/3} \quad (37)$$

$$j_m = \frac{h_{d,o}}{G_{a,max}} Sc_a^{2/3} \quad (38)$$

4. Results and discussion

Fig. 3(a) shows the fin efficiency for circular fin under fully dry, fully wet and partially wet conditions. The fully dry fin efficiency is obtained from Schmidt [24] and Kern and Kraus [23]. Note that the result from Schmidt [24] is an approximation to Kern and Kraus's result. For dry fin efficiency, the Schmidt approximation gives considerably good agreement with that of Kern and Kraus [23]. The calculations are in line with those reported by Hong and Webb [25] who also compares the fin efficiency calculated by Schmidt and Kern and Kraus. They found the deviation is less than 2% when $M_m(r_o - r_i) < 1.5$. The fully wet fin efficiency is obtained from McQuiston [26], Threlkeld [21], and Wang et al. [7]. The fin efficiency obtained from McQuiston [26] is based on the temperature difference

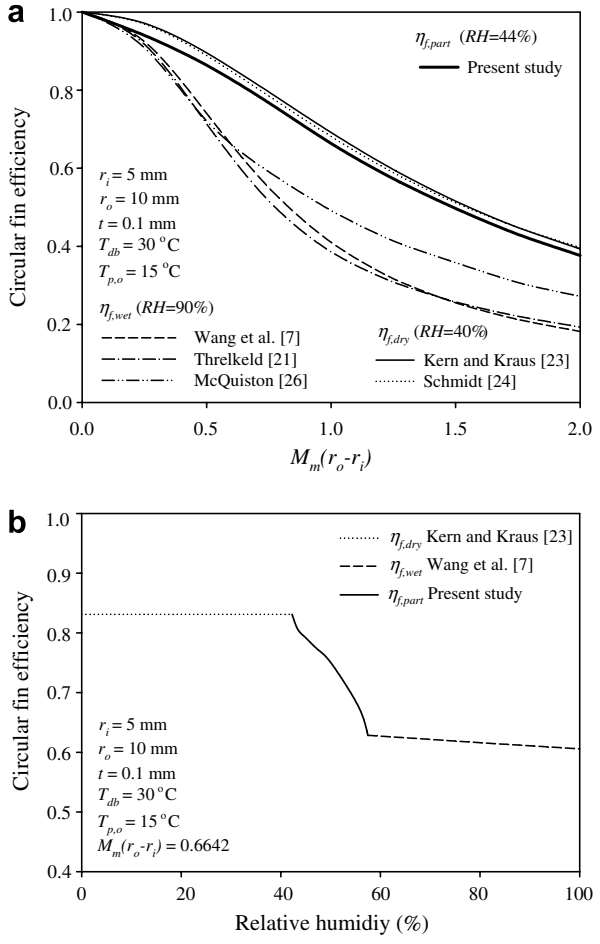

Fig. 3. Comparison of the fin efficiency with different authors of this study. (a) Circular fin efficiency plotted against $M_m(r_o - r_i)$. (b) Circular fin efficiency vs. relative humidity at $M_m(r_o - r_i) = 0.6642$.

but the fin efficiency obtained from Threlkeld [21] and Wang et al. [7] are based on the enthalpy difference. There are some ambiguities on determination of the wet fin efficiency. Webb and Kim [27] believed the McQuiston's approach is incorrect. Detailed discussions about this difference can be found from Lin et al. [28]. The partially wet fin efficiency is obtained from Eq. (27) is also shown in the figure. The presented partially wet fin efficiency is higher than the fully wet fin efficiency but is lower than the fully dry fin efficiency. The influence of the relative humidity on the partially wet fin efficiency is shown in Fig. 3(b). The fully dry fin efficiency is independent of relative humidity and the fully wet fin efficiency decreases very slightly with the rise of humidity. The results are analogous to Wu and Bong's results [29]. Calculations of the fully wet fin efficiency are based on the following equations [7]:

$$\eta_{f,wet} = \frac{2r_i}{M_T(r_o^2 - r_i^2)} \times \left[\frac{K_1(M_T r_i) I_1(M_T r_o) - K_1(M_T r_o) I_1(M_T r_i)}{K_1(M_T r_o) I_0(M_T r_i) + K_0(M_T r_i) I_1(M_T r_o)}\right] \quad (39)$$

$$\eta_{f,wet} = \frac{i_{a,m} - i_{s,f,m}}{i_{a,m} - i_{s,f,b}} \quad (40)$$

For a given dry-bulb temperature, the enthalpy increases slightly with the rise of relative humidity. Hence, it is expected that the enthalpy-based fin efficiency will decrease slightly. However, when $M_m(r_o - r_i)$ is low, the fully wet fin efficiency is almost constant. The partially wet fin efficiency decreases with the increase of the relative humidity from the fully dry fin efficiency to the fully wet fin efficiency. Rosario and Rahman [30] presented the partially wet fin efficiency for circular fin as

$$\eta_{f,part} = \left(\frac{r^{*2}}{r_o^2}\right)\eta_{f,dry} + \left(1 - \frac{r^{*2}}{r_o^2}\right)\eta_{f,wet} \quad (41)$$

However, the partially wet fin efficiency obtained from Eq. (41) cannot be used directly with the enthalpy-based reduction method such as that of Threlkeld's method. This is because that calculation of the partially wet fin efficiency involves fully dry and fully wet portions. The former involves only sensible heat transfer obtained from temperature difference whereas the latter includes both sensible and latent heat transfer termed as enthalpy difference. Thus it can not be applied based on the enthalpy difference alone. Likewise, for partially wet condition, it may be also not applicable for the equivalent dry-bulb temperature method [31] due to the heat transfer rate of this method is only calculated from the equivalent dry-bulb temperature difference. The last method for obtaining the heat transfer rate is dividing the heat transfer into two parts (one part for fully dry condition and the other part for fully wet condition). However, the partially wet fin efficiency will not be appeared in the calculation. This is because the fully dry fin efficiency is in the dry part and the fully wet fin

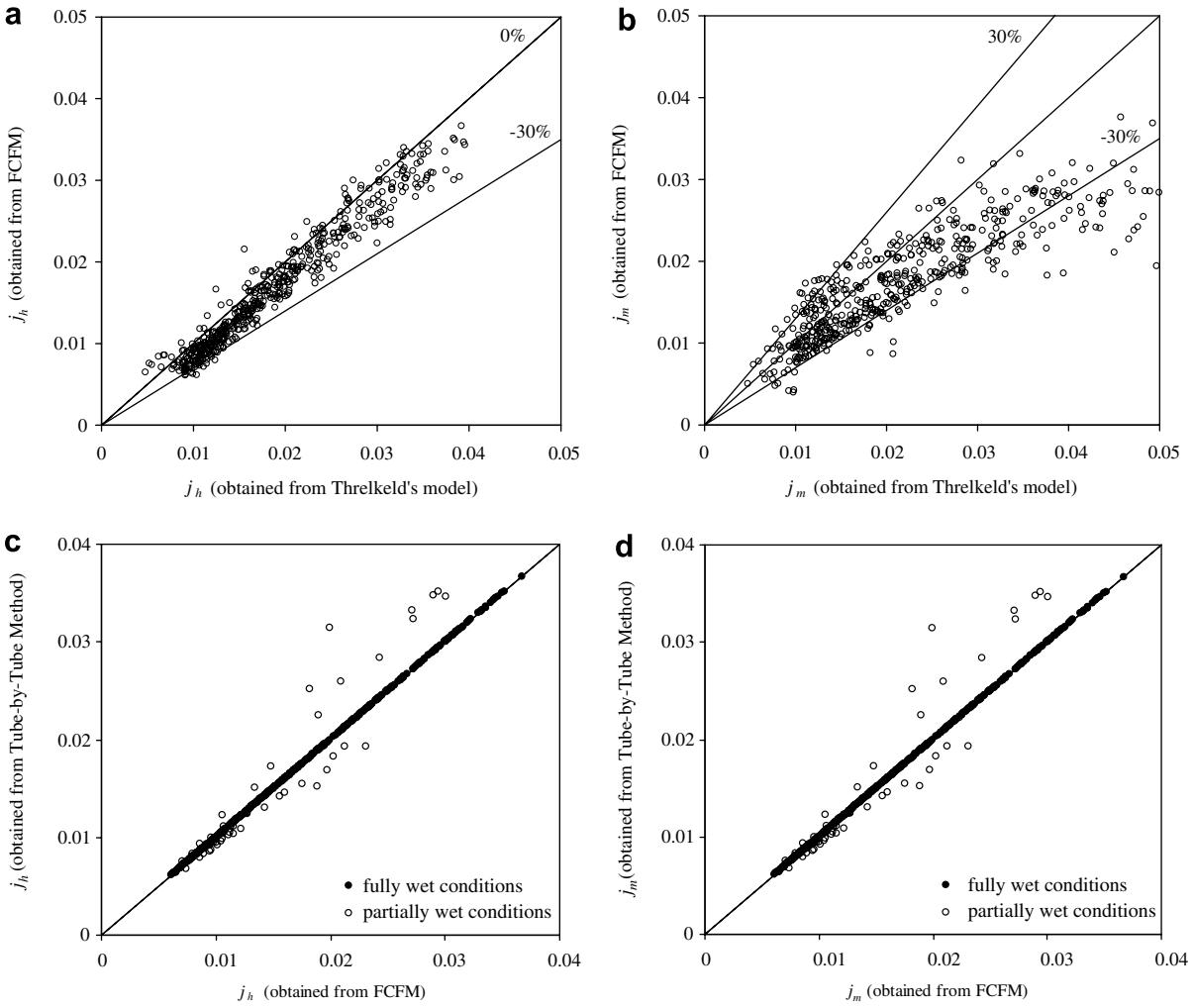

Fig. 4. Comparison of j_h and j_m between the proposed method and another reduction method. (a) j_h, FCFM vs. lumped Threlkeld's method. (b) j_m, FCFM vs. lumped Threlkeld's method. (c) j_h, FCFM vs. Tube-by-Tube method. (d) j_m, FCFM vs. Tube-by-Tube method.

efficiency is in the wet part. In that regard, we propose a new equation for obtaining the partially wet fin efficiency for the application based on the enthalpy difference.

The heat and mass transfer performances of the plain fin-and-tube heat exchangers are given in terms of the dimensionless parameters j_h and j_m, respectively. Test results are first compared with the original Threlkeld method. The comparisons are shown in Fig. 4(a) and (b). For the heat transfer performance, one can see in Fig. 4(a) that the original lumped approach is in fair agreement with the present discretized approach (86% of j_h within −30% to 0%). However, the j_h obtained by FCFM is slightly lower than those obtained by the Threlkeld method. There are two reasons for this result. The first one is because the j_h obtained by FCFM is based on discretized approach. In addition, the original Threlkeld method is applicable for fully wet surface only. For those data that are in partially wet conditions, an underestimation of the wet fin efficiency by the lumped Threlkeld method gives rise to a higher heat transfer coefficient, thereby yielding a higher j_h value accordingly. For the reduced results of the mass transfer performance shown in Fig. 4(b), one can see a much larger departure of the original Threlkeld method relative to the present FCFM (75% of j_m within −30% to 30%). This is attributed to the original Threlkeld method being more suitable for counter flow arrangements. By comparison with the Tube-by-Tube method presented by the present authors [11] as shown in Fig. 4(c) and (d), the heat and mass transfer coefficients obtained by FCFM for the fully wet conditions is equal to those obtained by the Tube-by-Tube method. However, for the partially wet conditions, the heat and mass transfer coefficients obtained by FCFM is different from those obtained from the Tube-by-Tube method. This is because the proposed FCFM method can take into account partially wet condition whereas the Tube-by-Tube method is more appropriate for fully wet condition.

A typical plot for examination of the influence of the inlet relative humidity and the fin pitch on the heat and mass transfer performances are shown in Fig. 5. As seen in Fig. 5(a) and (b), the heat transfer performance is relatively insensitive to the inlet relative humidity and fin pitch

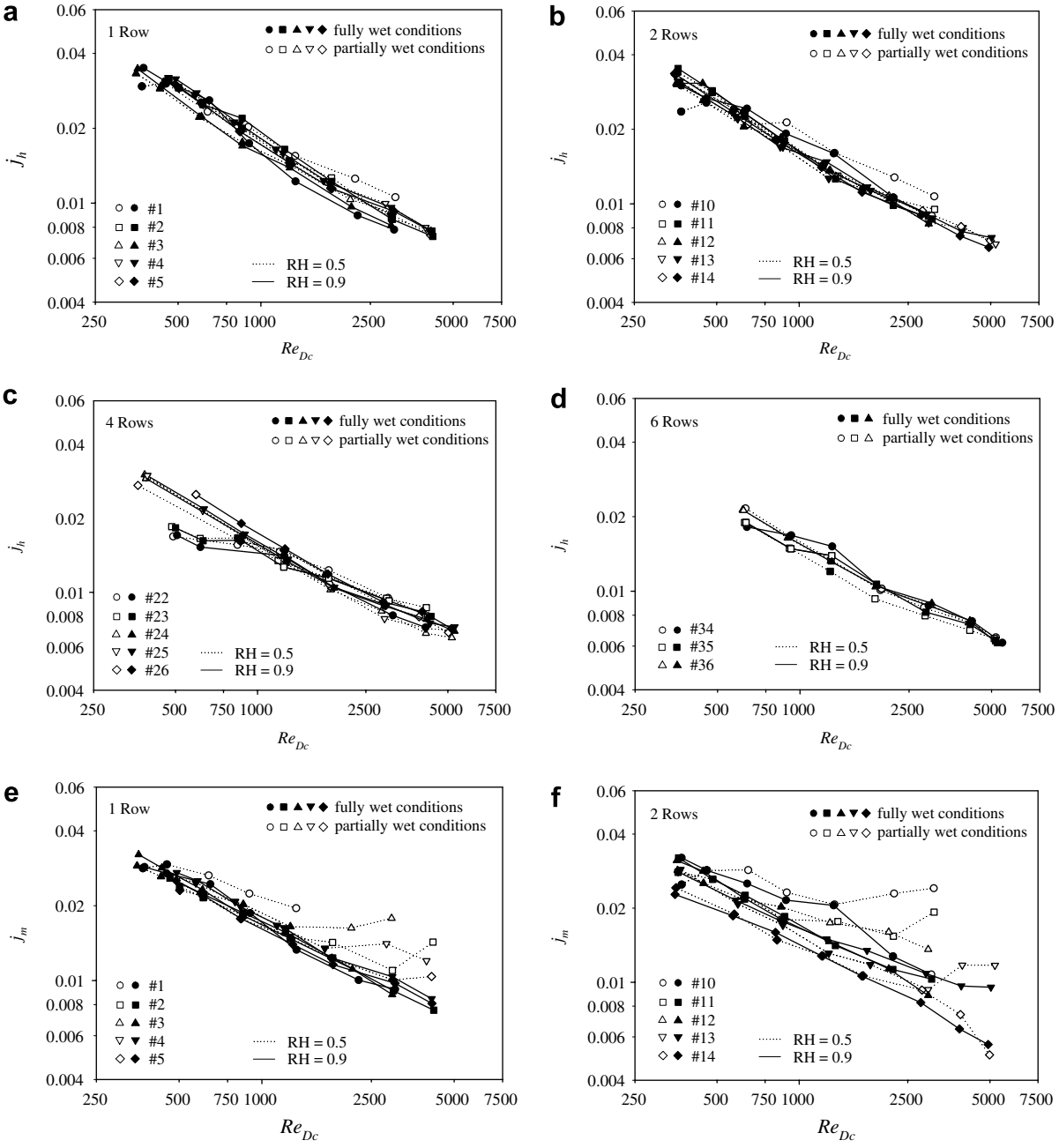

Fig. 5. Heat and mass transfer performances vs. Re_{Dc} for 1, 2, 4 and 6 rows configuration. (a) j_h, $N = 1$; (b) j_h, $N = 2$; (c) j_h, $N = 4$; (d) j_h, $N = 6$; (e) j_m, $N = 1$ and (f) j_m, $N = 2$.

for both $N = 1$ or $N = 2$. For the influence of fin pitch on the heat transfer performance having $N = 1$ or $N = 2$, the results are different from those in fully dry conditions as reported from Wang and Chi [18]. Based on the numerical simulation by Torikoshi et al. [32], they found that the vortex forms behind the tube can be suppressed and the entire flow region can be kept steady and laminar when the fin pitch is small enough. A further increase of fin pitch would result in a noticeable increase of cross-stream width of vortex region behind the tube. As a result, lower heat transfer performance is seen for larger fin pitch for 1-row configuration, indicating a detectable influence of fin pitch. However, it can be seen that the effect of fin pitch on the heat transfer performance is comparatively small for the wet fin surface. Apparently it is attributed to the presence of condensate that provides a good air flow mixing even at a larger fin pitch. In fact, the difference in heat transfer performance becomes even more negligible when the number of tube row is increased. With the increase of the number of tube rows, the condensate blow-off phenomenon from preceding row is blocked by the subsequent row. In that regard, the influence of relative humidity on the mass transfer performance becomes less profound and is deferred to an even higher Reynolds number ($Re_{Dc} > 2000$). Analogous results

(the influence of relative humidity and fin spacing on the heat and mass transfer performance) are obtained when the number of tube rows is further increased to 4 or 6 (Fig. 5(c) and (d)). The results agree with those reported by Wang et al. [7]. They reported negligible influence of fin pitch and inlet conditions on the heat transfer performance of a plain fin geometry when $N = 4$. The decrease of geometrical influences on the heat and mass transfer with the rising number of tubes can be made clear from a previous flow visualization study using scale-up fin-and-tube heat exchangers [33]. Their flow visualization experiment shows the injected dye in front of the first tube row hits the round tube and twists and swirls to the subsequent row. A clear horseshoe vortex is shown in front of the tube. The strength of the vertical motion is apparently stronger near the first row when compared to the second and third row. The strength of the swirled motion decays markedly with increasing rows. As a consequence, the associated influences of geometries become less profound. In addition, for $N \geqslant 4$, the sensible heat transfer coefficient is about the same as those of fully wet condition even the fin surface is partially wet.

As seen in Fig. 5(e) and (f), the influence of inlet relative humidity on the mass transfer characteristics is rather small when the fin spacing is sufficiently large (>2.0 mm). However, at a smaller fin spacing (samples #1, #2, #10, and #11) one can observe a slight decrease of j_m when the inlet relative humidity is increased from 50% to 90%. The slight decrease of mass transfer performance with inlet relative humidity at the dense fin spacing may be associated with the condensate retention phenomenon. Yoshii et al. [34] conducted a flow pattern observation about the air flow across tube bank, their results indicating that the blockage of the tube rows by the condensate retention may hinder the performance of the heat exchangers. Thus, one can see a slight drop of mass transfer performance. However, a considerable increase of mass transfer performance when $RH = 0.5$ and $Re_{Dc} > 1000$ is encountered. This is attributed to the blow-off condensate by flow inertia which makes more zoom for water vapor to condense along the surface.

It is obvious from the shown test results that no single curve can be expected to describe the complex behaviors for both j_h and j_m factors. As a result, by using a multiple linear regression technique in a practical range of experimental data ($300 < Re_{Dc} < 5500$), the appropriate correlation forms of j_h, j_m and R for the present data are

$N = 1$ (fully wet conditions)

$$j_{h,1,f} = 0.5284\left(\frac{S_p}{D_c}\right)^{0.5440}\varepsilon^{0.7519} \times Re_{Dc}^{\left(0.1001\frac{Sp}{Dc}-0.06529\frac{Pl}{Dc}-0.06752\frac{Pt}{Dc}-0.3734\right)} \quad (42)$$

$$j_{m,1,f} = 0.2143\left(\frac{S_p}{D_c}\right)^{1.3964}\varepsilon^{1.2298} \times Re_{Dc}^{\left(-0.2240\frac{Sp}{Dc}-0.1111\frac{Pl}{Dc}-0.06472\frac{Pt}{Dc}-0.08751\right)} \quad (43)$$

$$R_{1,f} = 2.2822\left(\frac{S_p}{D_c}\right)^{-0.8094}\varepsilon^{-0.4754} \times Re_{Dc}^{\left(0.2953\frac{Sp}{Dc}+0.04795\frac{Pl}{Dc}-0.001037\frac{Pt}{Dc}-0.2842\right)} \quad (44)$$

$N = 1$ (partially wet conditions, $0.65 < \frac{A_w}{A_o} < 1$)

$$j_{h,1,p} = j_{h,1,f}\left(\frac{S_p}{D_c}\right)^{-1.1918}\left(\frac{A_w}{A_o}\right)^{-1.1861} \times Re_{Dc}^{\left(1.0816\frac{Sp}{Dc}-0.06438\frac{Pl}{Dc}-0.1133\frac{Pt}{Dc}-0.05124\right)} \quad (45)$$

$$j_{m,1,p} = j_{m,1,f}\left(\frac{S_p}{D_c}\right)^{-1.3803}\left(\frac{A_w}{A_o}\right)^{-1.3489} \times Re_{Dc}^{\left(1.4155\frac{Sp}{Dc}-0.09474\frac{Pl}{Dc}-0.1092\frac{Pt}{Dc}-0.0791\right)} \quad (46)$$

$$R_{1,p} = R_{1,f}\left(\frac{S_p}{D_c}\right)^{0.3374}\left(\frac{A_w}{A_o}\right)^{0.2458} \times Re_{Dc}^{\left(-0.4613\frac{Sp}{Dc}+0.03085\frac{Pl}{Dc}+0.009432\frac{Pt}{Dc}+0.05053\right)} \quad (47)$$

$N > 1$ (fully wet conditions)

$$j_{h,N,f} = j_{h,1,f}N^{0.2310}\left(\frac{S_p}{D_c}\right)^{(-0.04426N-0.08561)}\varepsilon^{(-0.1407N-0.08005)} \times Re_{Dc}^{\left(0.02940N-0.1308\frac{Sp}{Dc}+0.03457\frac{Pl}{Dc}+0.04793\frac{Pt}{Dc}-0.1560\right)} \quad (48)$$

$$j_{m,N,f} = j_{m,1,f}N^{-0.01884}\left(\frac{S_p}{D_c}\right)^{(-0.06725N-1.4424)}\varepsilon^{(-0.1664N-0.7121)} \times Re_{Dc}^{\left(0.04525N+0.3173\frac{Sp}{Dc}+0.09050\frac{Pl}{Dc}+0.08353\frac{Pt}{Dc}-0.5101\right)} \quad (49)$$

$$R_{N,f} = R_{1,f}N^{0.2393}\left(\frac{S_p}{D_c}\right)^{(0.02390N+1.2426)}\varepsilon^{(0.03211N+0.5501)} \times Re_{Dc}^{\left(-0.01833N-0.4047\frac{Sp}{Dc}-0.05055\frac{Pl}{Dc}-0.03018\frac{Pt}{Dc}+0.3260\right)} \quad (50)$$

$N > 1$ (partially wet conditions, $0.44 < \frac{A_w}{A_o} < 1$)

$$j_{h,N,p} = j_{h,N,f}N^{-0.07957}\left(\frac{S_p}{D_c}\right)^{(-0.06148N+0.07271)}\left(\frac{A_w}{A_o}\right)^{(0.03322N-0.3148)} \times Re_{Dc}^{\left(-0.00885N+0.06733\frac{Sp}{Dc}+0.006928\frac{Pl}{Dc}+0.005305\frac{Pt}{Dc}-0.02962\right)} \quad (51)$$

$$j_{m,N,p} = j_{m,N,f}N^{0.09450}\left(\frac{S_p}{D_c}\right)^{(-0.1850N+0.5475)}\left(\frac{A_w}{A_o}\right)^{(0.2970N-1.1704)} \times Re_{Dc}^{\left(-0.03918N+0.06049\frac{Sp}{Dc}-0.00591\frac{Pl}{Dc}+0.02891\frac{Pt}{Dc}+0.03228\right)} \quad (52)$$

$$R_{N,p} = R_{N,f}N^{-0.4103}\left(\frac{S_p}{D_c}\right)^{(0.09196N-0.4592)}\left(\frac{A_w}{A_o}\right)^{(-0.2132N+0.6466)} \times Re_{Dc}^{\left(0.03407N+0.01464\frac{Sp}{Dc}+0.005748\frac{Pl}{Dc}-0.01564\frac{Pt}{Dc}-0.06849\right)} \quad (53)$$

Detailed comparison of the proposed correlation against the experimental data is shown in Fig. 6. It is found that Eqs. (42) and (48) can describe 93.45% of j_h for fully wet conditions within ±10% and Eqs. (45) and (51) can describe 91.51% of j_h for partially wet conditions within ±10%. Eqs. (43) and (49) can describe 93.45% of j_m for fully wet conditions within ±15% and Eqs. (46) and (52) can describe 87.26% of j_m for partially wet conditions within ±15%. Eqs. (44) and (50) can describe 98.26% of R for fully wet conditions within ±15% and Eqs. (47)

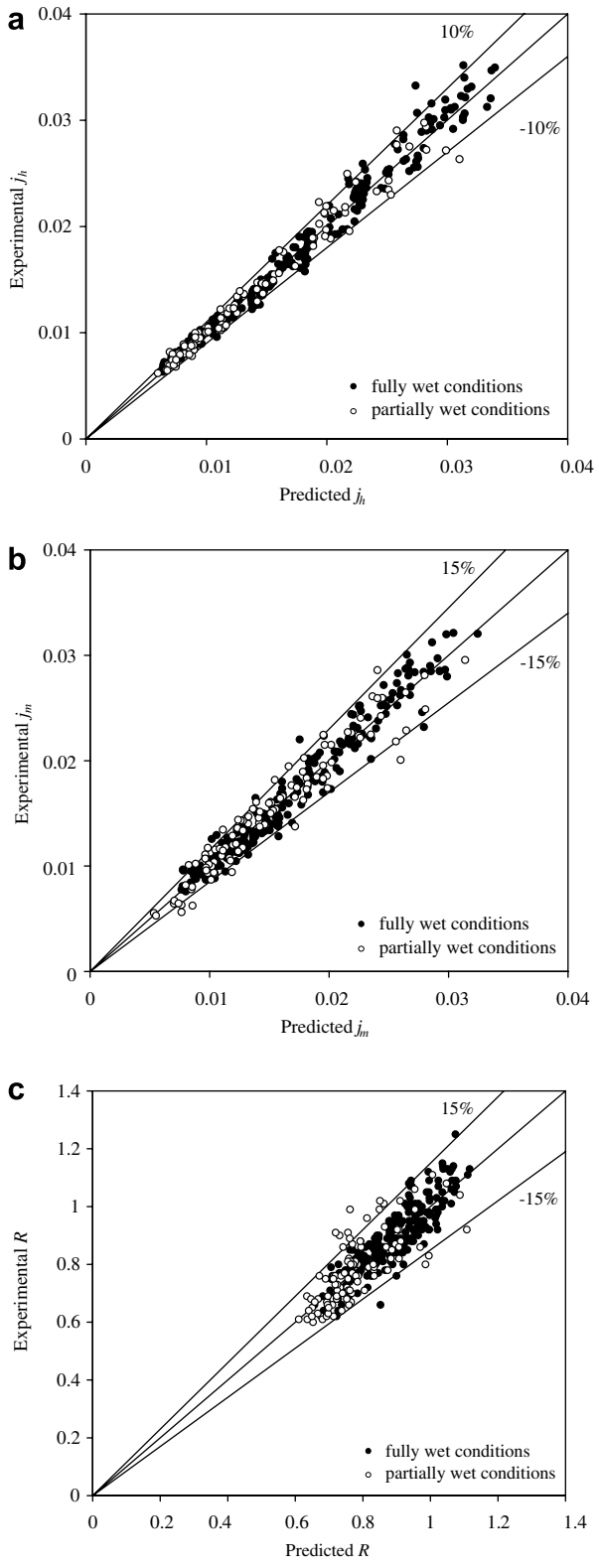

Fig. 6. Comparison between the proposed correlations against experimental data. (a) j_h, (b) j_m and (c) R.

and (53) can describe 88.89% of R for partially wet conditions within ±15%.

5. Conclusions

This study experimentally examines the heat and mass transfer characteristics of 36 fin-and-tube heat exchangers having plain fin geometry. On the basis of previous discussions, the following conclusions are made:

1. A FCFM is proposed in this study for reducing the test results. It is found that the reduced results for the sensible heat transfer performance by the present method are insensitive to changes of inlet humidity. Effect of fin pitch on the mass transfer performance is rather small when fin pitch is sufficiently large (>2.0 mm). However, at a small fin pitch, j_m slightly decreases when the relative humidity is increased.
2. Unlike those tested in fully dry conditions, the sensible heat transfer performance under dehumidification is comparatively independent of the fin pitch. This is because the presence of condensate plays a role in altering the air flow pattern within the heat exchanger, resulting in better mixing characteristics. For $N \geqslant 4$, the sensible heat transfer coefficient is about the same even the fin surface is partially wet.
3. For 1 and 2 rows configurations, the effect of relative humidity on the mass transfer performance becomes more pronounced when partially wet condition takes place.
4. A correlation is proposed for the present plain fin configuration. This correlation can describe 93.45% of j_h for fully wet conditions within ±10% and 91.51% of j_h for partially wet conditions within ±10% and can correlate 93.45% of j_m for fully wet conditions within ±15% and 87.26% of j_m for partially wet conditions within ±15%.

Acknowledgements

The authors are indebted to the Thailand Research Fund (TRF) and the Energy R&D foundation funding from the Bureau of Energy of the Ministry of Economic Affairs, Taiwan for supporting this study.

References

[1] F.C. McQuiston, Heat mass and momentum transfer data for five plate-fin tube transfer surface, ASHRAE Trans. Part 1 84 (1978) 266–293.
[2] F.C. McQuiston, Correlation of heat mass and momentum transport coefficients for plate-fin-tube heat transfer surfaces with staggered tubes, ASHRAE Trans. Part 1 84 (1978) 294–309.
[3] D.R. Mirth, S. Ramadhyani, Prediction of cooling-coils performance under condensing conditions, Int. J. Heat Fluid Flow 14 (4) (1993) 391–400.
[4] D.R. Mirth, S. Ramadhyani, Correlations for predicting the air-side Nusselt numbers and friction factors in chilled-water cooling coils, Exp. Heat Transfer 7 (1994) 143–162.
[5] W.L. Fu, C.C. Wang, C.T. Chang, Effect of anti-corrosion coating on the thermal characteristics of a louvered finned heat exchanger under

dehumidifying condition, Adv. Enhanced Heat/Mass Transfer Energy Efficiency, ASME HTD-vol. 320/PID-vol. 1 (1995) 75–81.
[6] Y. Seshimo, K. Ogawa, K. Marumoto, M. Fujii, Heat and mass transfer performances on plate fin and tube heat exchangers with dehumidification, Trans. JSME 54 (499) (1988) 716–721.
[7] C.C. Wang, Y.C. Hsieh, Y.T. Lin, Performance of plate finned tube heat exchangers under dehumidifying conditions, J. Heat Transfer 119 (1997) 109–117.
[8] J.L. Lage, Tube-to-tube heat transfer degradation effect finned tube heat exchangers, Numer. Heat Transfer: Part A: Appl. 39 (4) (2001) 321–337.
[9] Y.C. Shih, Numerical study of heat transfer performance on the air side of evaporator for a domestic refrigerator, Numer. Heat Transfer: Part A: Appl. 44 (8) (2003) 851–870.
[10] M. Tutar, M. Akkoca, Numerical analysis of fluid flow and heat transfer characteristics in three-dimensional plate fin-and-tube heat exchangers, Numer. Heat Transfer: Part A: Appl. 46 (3) (2004) 301–321.
[11] W. Pirompugd, S. Wongwises, C.C. Wang, A tube-by-tube reduction method for simultaneous heat and mass transfer characteristics for plain fin-and-tube heat exchangers in dehumidifying conditions, Heat Mass Transfer 41 (8) (2005) 756–765.
[12] W. Pirompugd, S. Wongwises, C.C. Wang, Simultaneous heat and mass transfer characteristics for wavy fin-and-tube heat exchangers under dehumidifying conditions, Int. J. Heat Mass Transfer 49 (2006) 132–143.
[13] Y. Xia, A.M. Jacobi, Air-side data interpretation and performance analysis for heat exchangers with simultaneous heat and mass transfer: wet and frosted surfaces, Int. J. Heat Mass Transfer 48 (2005) 5089–5102.
[14] ASHRAE Standard 41.2, Standard methods for laboratory air-flow measurement, American Society of Heating, Refrigerating and Air-Conditioning Engineers, Inc., Atlanta GA, 1987.
[15] ASHRAE Standard 41.1, Standard method for temperature measurement, American Society of Heating, Refrigerating and Air-Conditioning Engineers, Inc., Atlanta, GA, 1986.
[16] ASHRAE Standard 33-78, Method of testing forced circulation air cooling and air heating coils, American Society of Heating, Refrigerating and Air-Conditioning Engineers, Inc., Atlanta, GA, 1978.
[17] R.J. Moffat, Describing the uncertainties in experimental results, Exp. Therm. Fluid Sci. 1 (1988) 3–17.
[18] C.C. Wang, K.U. Chi, Heat transfer and friction characteristics of plain fin-and-tube heat exchangers: part I: new experimental data, Int. J. Heat Mass Transfer 43 (2000) 2681–2691.
[19] T.R. Bump, Average temperatures in simple heat exchangers, ASME J. Heat Transfer 85 (2) (1963) 182–183.
[20] R.J. Myers, The Effect of Dehumidification on the Air-side Heat Transfer Coefficient for a Finned-tube Coil, M.S. Thesis, University of Minnesota, Minneapolis, 1967.
[21] J.L. Threlkeld, Thermal Environmental Engineering, Prentice-Hall, New York, NY, 1970.
[22] V. Gnielinski, New equation for heat and mass transfer in turbulent pipe and channel flow, International Chemical Engineering 16 (1976) 359–368.
[23] D.Q. Kern, A.D. Kraus, Extended Surface Heat Transfer, McGraw-Hill, New York NY, 1972.
[24] T.E. Schmidt, Heat transfer calculations for extended surfaces, Refrige. Eng. 49 (1949) 351–357.
[25] T.K. Hong, R.L. Webb, Calculation of fin efficiency for wet and dry fins, Int. J. HVAC&R Res. 2 (1) (1996) 27–41.
[26] F.C. McQuiston, Fin efficiency with combined heat and mass transfer, ASHRAE Trans. Part 1 81 (1975) 350–355.
[27] R.L. Webb, N.H. Kim, Principles of Enhanced Heat Transfer, second ed., Taylor & Francis, New York, 2005, p. 197.
[28] Y.T. Lin, K.C. Hsu, Y.J. Chang, C.C. Wang, Performance of rectangular fin in wet conditions: visualization and wet fin efficiency, ASME J. Heat Transfer 123 (2001) 836–927.
[29] G. Wu, T.Y. Bong, Overall efficiency of a straight fin with combined heat and mass transfer, ASHRAE Trans. 100 (1) (1994) 367–374.
[30] L. Rosario, M.M. Rahman, Analysis of heat transfer in a partially wet radial fin assembly during dehumidification, Int. J. Heat Fluid Flow 20 (1999) 642–648.
[31] J. Wang, E. Hihara, Prediction of air coil performance under partially wet and totally wet cooling conditions using equivalent dry-bulb temperature method, Int. J. Refrige. 26 (2003) 293–301.
[32] K. Torikoshi, G. Xi, Y. Nakazawa, H. Asano, Flow and heat transfer performance of a plate-fin and tube heat exchanger (1st report: effect of fin pitch), 10th Int. Heat Transfer Conf. 1994 paper 9-HE-16, 1994, pp. 411–416.
[33] C.C. Wang, J. Lo, Y.T. Lin, C.S. Wei, Flow visualization of annular and delta winglet vortex generators in fin-and-tube heat exchanger application, Int. J. Heat Mass Transfer 45 (2002) 3803–3815.
[34] T. Yoshii, M. Yamamoto, M. Otaki, Effects of dropwise condensate on wet surface heat transfer of air cooling coils, in: Proceedings of the 13th International Congress of Refrigeration, 1973, pp. 285–292.